

Towards the Experimental Decomposition Rate of Carbonic Acid (H₂CO₃) in Aqueous Solution

Christofer S. Tautermann, Andreas F. Voegelé, Thomas Loerting, Ingrid Kohl, Andreas Hallbrucker, Erwin Mayer, and Klaus R. Liedl*^[a]

Abstract: Dry carbonic acid has recently been shown to be kinetically stable even at room temperature. Addition of water molecules reduces this stability significantly, and the decomposition (H₂CO₃ + *n*H₂O → (*n*+1)H₂O + CO₂) is extremely accelerated for *n*=1, 2, 3. By including two water molecules, a reaction rate that is a factor of 3000 below the experimental one (10 s⁻¹) at room temperature was found. In order to further remove the gap between experiment and theory, we increased the number of water molecules involved to 3 and took into consideration different mechanisms for thorough elucidation

of the reaction. A mechanism whereby the reaction proceeds via a six-membered transition state turns out to be the most efficient one over the whole examined temperature range. The determined reaction rates approach experimental values in aqueous solution reasonably well; most especially, a significant increase in the rates in comparison to the decomposition reaction with

fewer water molecules is found. Further agreement with experiment is found in the kinetic isotope effects (KIE) for the deuterated species. For water-free carbonic acid, the KIE (i.e., *k*_{H₂CO₃}/*k*_{D₂CO₃}) for the decomposition reaction is predicted to be 220 at 300 K, whereas it amounts to 2.2–3.0 for the investigated mechanisms including three water molecules. This result is therefore reasonably close to the experimental value of 2 (at 300 K). These KIEs are in much better accordance with the experiment than the KIE for decomposition with fewer water entities.

Keywords: ab initio calculations • carbonic acid • environmental chemistry • isotope effects • kinetics • proton transfer reactions

Introduction

In a preliminary communication we reported on the influence of additional water molecules on the decomposition rate of carbonic acid.^[1] Here we provide the details of the reactions investigated formerly and a further extension to another additional water entity in this reaction.

Carbonic acid is known to be one of the molecules that have a fundamental impact on biological systems.^[2–5] The hydration equilibrium is well examined experimentally,^[6–10] and there have been many attempts to interpret it theoretically.^[11–16] We have studied the influence of water molecules on the kinetic stability of carbonic acid by means of quantum chemistry.^[1] We concluded that dry carbonic acid in the gas phase is kinetically stable, even at room temperature. Stored in liquid nitrogen (at a temperature of 77 K), the reaction rate of the decomposition amounts to 10⁻²⁸ s⁻¹, corresponding to a half

life of 2 × 10²⁰ years. Carbonic acid in the gas phase consists of a mixture of monomers and dimers, with a temperature depending ratio.^[17] Whereas the dimer has been calculated to be of similar energy with respect to its constituents,^[13] the monomer is thermodynamically unstable and was believed to decompose immediately.^[11, 14, 18]

Despite the usual belief in the nonexistence of carbonic acid, chemists have generated and isolated the pure compound either by proton irradiation of H₂O/CO₂ ice mixtures^[19] and solid carbon dioxide^[20] or by protonation at low temperatures of carbonate or bicarbonate.^[21] The formation of carbonic acid in H₂O/CO₂ ices could also be achieved by UV irradiation but to a smaller extent, limited by the penetration of the photons into the ice.^[22] Furthermore, the stability in the gas phase at temperatures around 200 K could be proved by sublimation and recondensation experiments.^[17]

This remarkable stability gives an indication of the astrophysical relevance of carbonic acid; H₂CO₃ is believed to be present on planets or comets.^[17] Especially, the planet Mars could provide the conditions necessary for the formation of solid carbonic acid with its frozen polar caps, which mainly consist of water and carbon dioxide,^[23, 24] and the absence of a magnetic field,^[25] in analogy to the experiments of Moore and Khanna.^[19, 22] Comparison of the infrared spectrum of the

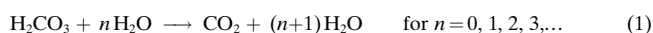
[a] Prof. Dr. K. R. Liedl, MMag. C. S. Tautermann, Mag. A. F. Voegelé, Dr. T. Loerting, Dr. I. Kohl, Prof. Dr. A. Hallbrucker, Prof. Dr. E. Mayer
Institute of General, Inorganic and Theoretical Chemistry
University of Innsbruck, Innrain 52a, 6020 Innsbruck (Austria)
Fax: (+43) 512-507-5144

Martian surface to laboratory spectra of H_2CO_3 suggests that carbonic acid is present.^[17, 23]

A more technical occurrence of carbonic acid is in steam reactors, where it is shown to be one of the contaminants that leads to corrosion of the working turbines.^[26] Generally, it appears in all water-based steam–condensate cycles of nuclear and fossil-fuel power plants and contributes to the corrosion of steam and return lines. Special analytical methods have been developed to quantify even very low concentrations of carbonic acid in steam.^[27] One way of attempting to understand the process of corrosion in these systems is to investigate the contributing reaction mechanisms, in which the formation of carbonic acid seems to be one of the key steps.

Due to the huge impact of the anhydride of carbonic acid, namely carbon dioxide, on the climate as a greenhouse gas, there are many attempts to remove it from the atmosphere.^[28] One method of CO_2 sequestration is to dispose it at the bottom of the oceans as solid CO_2 ,^[29] where huge amounts of carbon already occur naturally in the form of solid carbon dioxide or carbonate.^[30] Before this disposal can be carried on a large scale, the impacts on maritime life have to be investigated.^[31] In ocean carbon-cycle models, the effect of CO_2 sequestration is investigated, and these models require knowledge of the equilibrium constant of the hydration equilibrium of carbon dioxide at many different conditions (temperature, pressure, salinity) in order to consider changes in the pH value.^[32]

However, the mechanisms of dehydration of carbonic acid in aqueous solution, and the reaction in the backward direction (that is the hydration of carbon dioxide to carbonic acid) were for a long time the subject of speculation.^[6, 33] By contrast, the reaction rates (9.2 s^{-1} – 14.6 s^{-1} at 18°C ^[7, 9] and 10 s^{-1} at 20°C ^[8] for the decomposition of carbonic acid) as well as the kinetic isotope effects ($k_{\text{H}_2\text{CO}_3}/k_{\text{H}_2\text{CO}_3} \approx 2$, i.e., the decomposition ratio of deuterated carbonic acid in deuterated water is twice as slow as carbonic acid in water^[6]) are well known. The main interest in previous studies was on the water-catalyzed decrease of the energy barrier.^[18] Additional water molecules thus have a very strong effect on the reaction rate, that is, the decay is tremendously accelerated by water mediated proton transfer, Equation (1).



We used this reaction as a starting point for a detailed investigation to get a better understanding of the processes taking place in aqueous solution.

Computational Methods

Theory: We have applied the variational approach to transition state theory (TST)^[34–41] including quantum chemical effects like tunneling and corner cutting in order to calculate the reaction rates. The potential energy surface (PES) was calculated at a lower level of theory by employing the hybrid density functional method B3LYP with the 6–31 + G(d) basis set. The minimum energy path (MEP), which is the

path of least energy connecting products and reactants in internal mass-weighted coordinates, was determined by using the Page–McIver method.^[42, 43] The step size was set to 0.05 Bohr, and every third step along the MEP harmonic frequencies was calculated.

The stationary points were determined at the CCSD(T)/aug-cc-pVDZ//MP2/aug-cc-pVDZ (for $n=0$ up to the aug-cc-pVTZ basis set) level of theory and for $n=0, 1$ we compared the energy differences with G2* values.^[44–46] The results of these high-level methods are in excellent agreement with each other as they deviate by less than 1 kcal mol^{-1} (see Table 2, below). Vibrational frequencies were determined at the B3LYP/aug-cc-pVDZ level of theory.

The PES was interpolated to the three high-level stationary points (i.e., the reactants, the transition state and the products) according to an interpolation scheme that also maps the harmonic frequencies and moments of inertia onto the high-level data.^[47]

Quantum chemical corrections were applied to the variational transition state theory (VTST). We used three different approaches for taking into account tunneling contributions in the framework of the semiclassical theory:^[48] 1) The zero-curvature tunneling approach (ZCT), which assumes that tunneling occurs only along the MEP, 2) the small-curvature tunneling approach^[39, 49] (SCT), which allows moderate corner-cutting along a curved MEP, and 3) the large-curvature tunneling approach^[37] (LCT), which leads to tunneling paths far off the MEP in the nonadiabatic region. As large curvature method we employed the LCG4 method to include anharmonicity in the tunneling calculations.^[50]

The first two methods do not require any information additionally to the MEP and the harmonic frequencies along it, but in the LCT method it is normally necessary (depending on the curvature of the MEP) to calculate more energy points in the region between the two branches of the MEP, that is, the so-called reaction swath. Whereas the ZCT method gives poor results for the tunneling correction, the other methods work well. As both the LCT and SCT methods perform well in quite different situations, mostly depending on the temperature and the masses of the atoms involved in the tunneling process, the optimum is to use the larger tunneling correction of the two. This is called the microcanonical-optimized multidimensional tunneling method,^[51] which is an excellent approach for including tunneling corrections over the full temperature range.

All stationary points were determined with the Gaussian98 package,^[52] and the kinetics calculations were performed with Polyrate^[53] and Gaussrate,^[54] this being an interface between Gaussian98 and Polyrate.

Mechanisms: For determining the kinetics of the reaction, it is necessary to investigate and understand the reaction mechanism thoroughly. In the case of the decay of carbonic acid, this mechanism is called water-mediated proton transfer.

This mechanism was found for other reactions as well, like the clockwise or counterclockwise movement of the protons in neutral cyclic water clusters^[55] as an example of synchronous transitions. Systems showing an asynchronous proton transition behavior are, for example, the hydration equilib-

rium of SO_3 ,^[56–59] which plays a very important role in atmospheric chemistry, as well as the competing hydration equilibrium of SO_2 ,^[56, 60] and the hydrolysis of N_2O_5 .^[61] Other examples of asynchronous transition behavior are the water-assisted tautomerizations of formamide^[62] and 7-azaindole,^[63, 64] which play a fundamental role in biological systems. The formamidine dimer has a concerted, synchronous proton transfer in the gas phase but a stepwise mechanism is followed in aqueous solution.^[65]

It is also necessary to use diffuse functions in order to get an adequate representation of the H bonds. When dealing with reaction dynamics it is crucial to know the energy barrier accurately in order to get reliable results. According to Eyring's theory of the activated complex,^[66–68] errors in the energy barrier of only $1.4 \text{ kcal mol}^{-1}$ lead to perturbations larger than one order of magnitude in the reaction rate at 300 K.

In addition, tunneling corrections have to be employed to conventional Transition State Theory in order to achieve accurate results in the reaction rates.^[35, 37–41, 69–71]

Results and Discussion

Reaction geometries and energetics: The geometries of the stationary points were optimized at the MP2/aug-cc-pVDZ level of theory (for the uncatalyzed case up to MP2/aug-cc-pVTZ level), and for $n=0, 1, 2$ good agreement with the geometries obtained by Nguyen et al.^[18] was found. For the $n=3$ case we determined several different reaction channels. Some of them could be excluded as having a too high reaction barrier. Therefore, the three pathways with the lowest barriers were chosen for further investigation. Channel (a) contains a six-membered transition state, channel (b) involves an eight-membered one, and channel (c) has a 10-membered one (Figure 1). Channel (a) can be seen to be similar to the

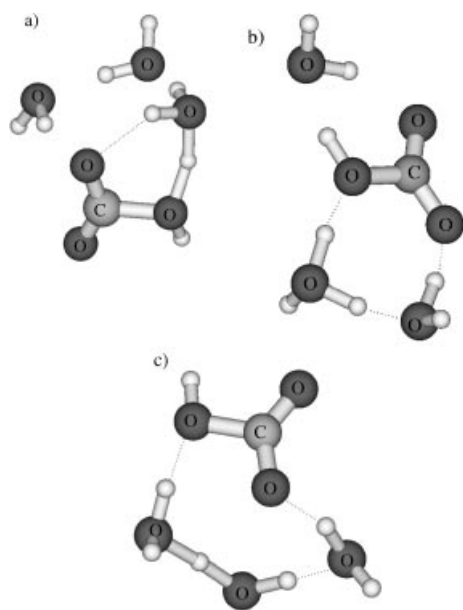


Figure 1. Transition states of the decomposition of carbonic acid catalyzed by three additional water molecules. a) transition state with a six-membered ring, b) with an eight-membered ring, and c) with a 10-membered ring.

decomposition reaction with one water molecule (i.e., $n=1$) and two “spectator” water entities, which are not actively involved in the proton transfer. The importance of these water molecules lies in their ability to microsolvate the system and, therefore, stabilize the transition state with respect to the reactants. This stabilization amounts to more than 6 kcal mol^{-1} (see Table 2, below) and leads to a strong enhancement of the reaction rate.

Similarly, channel (b) may be seen as the decomposition reaction with two additional water molecules (i.e., $n=2$) and one “spectator” water entity. The lowering of the energy barrier due to the spectator is only $1.3 \text{ kcal mol}^{-1}$ in this case, and thus leads to no strong acceleration of the reaction.

Finally, channel (c) might be seen as a direct extension of the mechanisms with fewer water entities (see Loerting et al.^[1]), because all the water molecules are actively involved in the proton transfer. At low level (B3LYP/6–31 + G(d)), this mechanism yields similar reaction rates as channel (a), but high-level treatment of the activation barrier reveals its kinetical inferiority. Although possessing comparable energy barriers at a low level of theory, at a high level channel (c) turns out to have a barrier $2.2 \text{ kcal mol}^{-1}$ higher and also significantly wider (see Figure 2, below).

The nature of all stationary points was verified by a harmonic vibrational frequency analysis, that is, the transition states are required to have one imaginary frequency, whereas the products and reactants must only possess real frequencies. Table 1 shows the imaginary frequencies of the transition states depending on n . Increasing the number of catalytic water molecules leads to a strong decrease in the magnitude of the imaginary frequencies. This, in turn, leads to strong differences in the influence of tunneling effects within the reactions. Even the crude Wigner approximation^[69] for the tunneling effect differs by more than one order of magnitude at low temperatures.

Table 1. Imaginary frequencies in cm^{-1} at the transition state of the decomposition reaction of carbonic acid assisted by $n=0, 1, 2, 3$ water entities.

n	B3LYP/aug-cc-pVDZ	MP2/aug-cc-pVDZ
0	1724i	1707i
1	1080i	1102i
2	570i	
3(a)	601i	
3(b)	463i	
3(c)	393i	

The energy barriers and the reaction energies of the decomposition reaction of carbonic acid ($\text{H}_2\text{CO}_3 + n\text{H}_2\text{O} \rightarrow (n+1)\text{H}_2\text{O} + \text{CO}_2$) were determined at the CCSD(T)/aug-cc-pVDZ//MP2/aug-cc-pVDZ level of theory (for the uncatalyzed system up to CCSD(T)/aug-cc-pVTZ//MP2/aug-cc-pVTZ level) and they are shown in Table 2. The energy values for $n=0, 1, 2$ are in very good agreement with those published by Nguyen et al.,^[18] especially, the energy barriers differ by less than 1 kcal mol^{-1} . For the $n=3$ case no data at a comparably high level were found in the literature. Due to the catalytic effect of additional water molecules, the

Table 2. Energy barrier and reaction energy of $\text{H}_2\text{CO}_3 + n\text{H}_2\text{O} \rightarrow (n+1)\text{H}_2\text{O} + \text{CO}_2$ at the CCSD(T)/aug-cc-pVDZ//MP2/aug-cc-pVDZ level of theory (for $n=0$ up to CCSD(T)/aug-cc-pVTZ//MP2/aug-cc-pVTZ level) and on the G2* level for $n=0, 1$. All values are in kcal mol^{-1} .

n	Method	Energy Barrier	Reaction Energy
0	CCSD(T)/VDZ	43.6 ^[a]	-9.1 ^[a]
	CCSD(T)/VTZ	43.9	-7.4
	G2*	44.8	-8.0
1	CCSD(T)/VDZ	27.1 ^[a]	-7.6 ^[a]
	G2*	27.7	-6.5
2	CCSD(T)/VDZ	24.0 ^[a]	-7.6 ^[a]
3(a)	CCSD(T)/VDZ	20.9	-8.2
3(b)	CCSD(T)/VDZ	22.7	-7.1
3(c)	CCSD(T)/VDZ	23.1	-9.6

[a] See ref. [1].

barrier decreases with the amount of water entities, whereas the reaction energy is only slightly influenced. While the first water entity lowers the barrier by about $16.5 \text{ kcal mol}^{-1}$, the addition of further water molecules has a lowering effect of less than $6.5 \text{ kcal mol}^{-1}$. This effect can be explained by the unfavorable geometry of the transition state of the uncatalyzed reaction. The four-membered ring suffers from being much more strained than the 6–10-membered rings of the catalyzed systems. The extent of the decrease of the barrier diminishes with each new water entity, so that the barrier height eventually becomes independent of the amount of water molecules, that is, convergence against the activation barrier in aqueous solution is achieved. Determining and working with the amount of water molecules necessary to reach bulk properties on a high level of quantum chemical methods goes beyond today's technical feasibility.

Reaction paths: Figure 2 shows the dual-level corrected minimum energy paths of the decomposition reaction of carbonic acid. The energy values of the stationary points have been mapped onto the CCSD(T)/aug-cc-pVDZ values (Table 2).

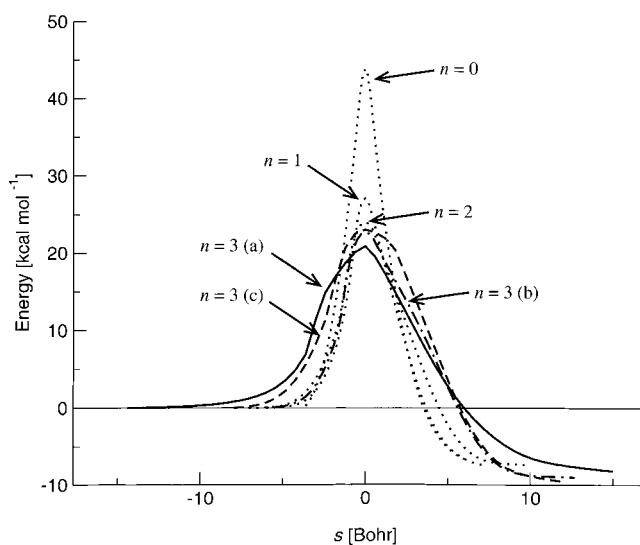


Figure 2. Dual-level corrected minimum energy paths of the reaction $\text{H}_2\text{CO}_3 + n\text{H}_2\text{O} \rightarrow (n+1)\text{H}_2\text{O} + \text{CO}_2$ depending on n . s is a metric path parameter along the minimum energy path, namely the reaction coordinate. Paths with $n=0, 1, 2$ were taken from Loerting et al.^[1]

As the reaction mechanisms with $n=0, 1, 2$ were discussed earlier,^[1] they will be reviewed briefly and we will then concentrate on the reaction mechanisms with three additional water molecules.

Reactions with $n=0, 1, 2$: In the case of the uncatalyzed reaction, one proton is transferred via a four-membered transition state. With $n=1$ two protons are moved, and the proton transfer is mediated by the additional water molecule. The protons do not move at the same time, so the transfer mechanism must be called asynchronous. As there are no local minima along the reaction path, but only one transition state, the proton transfer is concerted, that is, energetically coupled. The transition state has a planar six-membered ring, which is considerably less strained than the four-membered ring in the uncatalyzed reaction. On adding another water molecule, the type of reaction remains the same—an asynchronous concerted proton transfer reaction—but the amount of protons being transferred rises to three. Again some strain may be relieved from the transition state, which contains an eight-membered ring with H-O-H angles near to 180° .

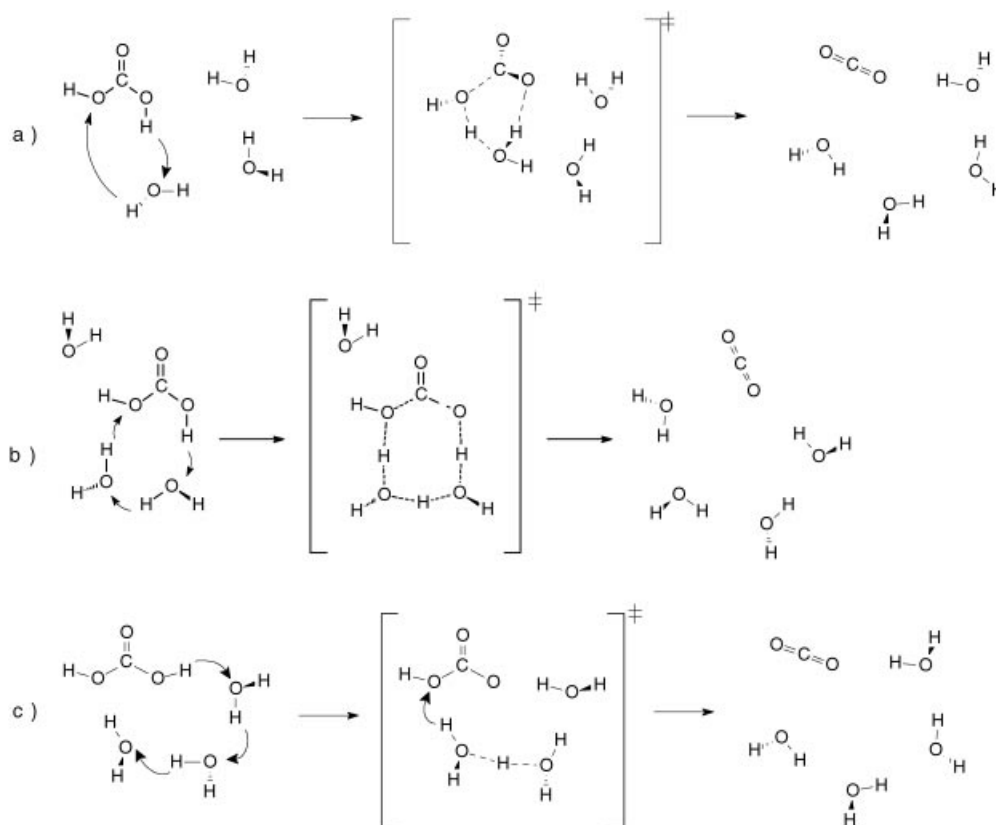
Reactions with $n=3$: Scheme 1 shows three different reaction channels that are proposed to be the most efficient ones for the dehydration reaction.

Again all reaction channels display a concerted asynchronous proton-transition behavior. Pathway (a) involves only one water entity directly into the proton shuttle mechanism whereas channel (b) needs two water molecules for a Grotthus-like proton-jumping mechanism and channel (c) employs all three water molecules for the proton mediation.

Channel (a), six-membered transition state: After the proton has moved apart from the carbonic acid, the transition state contains a strongly polarized hydronium ion like substructure. Only one water molecule is actually involved in the proton transition, but the two other water molecules are essential for lowering the activation-energy barrier. The other water molecules assist the abstraction of the proton from the carbonic-acid oxygen in the first step of the reaction and contribute to the stabilization of the H_3O^+ -like species in the transition state.

The analogy to the reaction of carbonic acid with one additional water entity can be seen. Ignoring the two “spectator” water molecules, the reaction mechanisms are essentially the same. The huge impact of these water molecules lies in their ability to stabilize the (very polar) transition state and thus lower the reaction barrier. The second benefit of these “spectators” is the polarization of the oxygen of the hydroxy group, which facilitates the abstraction of the hydrogen.

Channel (b), eight-membered transition state: In analogy to reaction channel (a), after the movement of the first proton a transition state is formed that contains an hydronium ion like substructure. In the subsequent steps, a proton from the hydronium ion like substructure is transferred to the other participating water molecule, from which a proton moves



Scheme 1. Stationary points of the three reaction channels with three additional water molecules.

back to the carbonic acid that has already decomposed into water and carbon dioxide by this stage of the reaction.

Once again one water acts as a “spectator”, stabilizing the polar transition species and facilitating the abstraction of the proton from the oxygen in the first step of the reaction. Without this water molecule the whole reaction is essentially the same as the decomposition reaction of carbonic acid with two water molecules.

Channel (c), 10-membered transition state: All three water molecules are actively involved in the proton transfer, as they form a hydrogen-bonded ring around which the protons can move in a Grotthus-like manner. Again the transition state is strongly polarized due to formation of a $H_5O_2^+$ -like species. Though the proton transfer is concerted, it is far from being synchronous; this results in a strong broadening of the energy barrier.

Figure 3 displays the imaginary frequencies of reactions (a), (b), and (c) along the reaction path. Each transfer of a single proton leads to a peak in the magnitude of the imaginary frequency. Hence, an asynchronous proton-transfer mechanism is observed in both cases. The peaks in the imaginary frequencies along the reaction path display very accurately the points in the reaction at which protons are transferred. Thus, the three reactions can easily be discriminated by just observing the imaginary frequency along the reaction path. In the case of channel (a) just two protons are transferred, in channel (b) three protons are seen to move, and in channel (c) four protons flip between neighboring oxygens. Another very

important fact can be deduced from Figure 4: as protons are able to tunnel through barriers quite easily it is advantageous if all protons are transferred near the top of the energy barrier in order to increase the tunneling correction. In the case of channels (a) and (b), the movement of the protons is located in the reaction path near the top of the barrier, whereas the transfer of the protons is widespread along the reaction path in channel (c). Thus we have significantly higher tunneling corrections for channels (a) and (b) in comparison with channel (c).

An important feature of all three different reaction channels is the fact that a polar transition state is formed. Thinking of the decomposition reaction in aqueous solution, this might have an enormous impact. As water acts as a polar solvent, these transition structures become stabilized, and a lowering of the reaction barrier is expected if polarized continuum models are applied. As no structural convergence of the geometries could be achieved by using the polarized continuum model (PCM) by Tomasi and co-workers,^[72] the PCM-method was applied to the gas-phase structures of the stationary points. When evaluating PCM(MP2/aug-cc-pVDZ)/MP2/aug-cc-pVDZ barriers, a lowering of between 1 and 5 kcal mol⁻¹ in the activation barrier is found in the three reaction channels. This would lead to an enhancement of the reaction rate of about 1–3 orders in magnitude and, therefore, approach the experimental decomposition rate in aqueous solution. One must be aware that these are just crude approximations, in particular concerning the geometry of the stationary points.

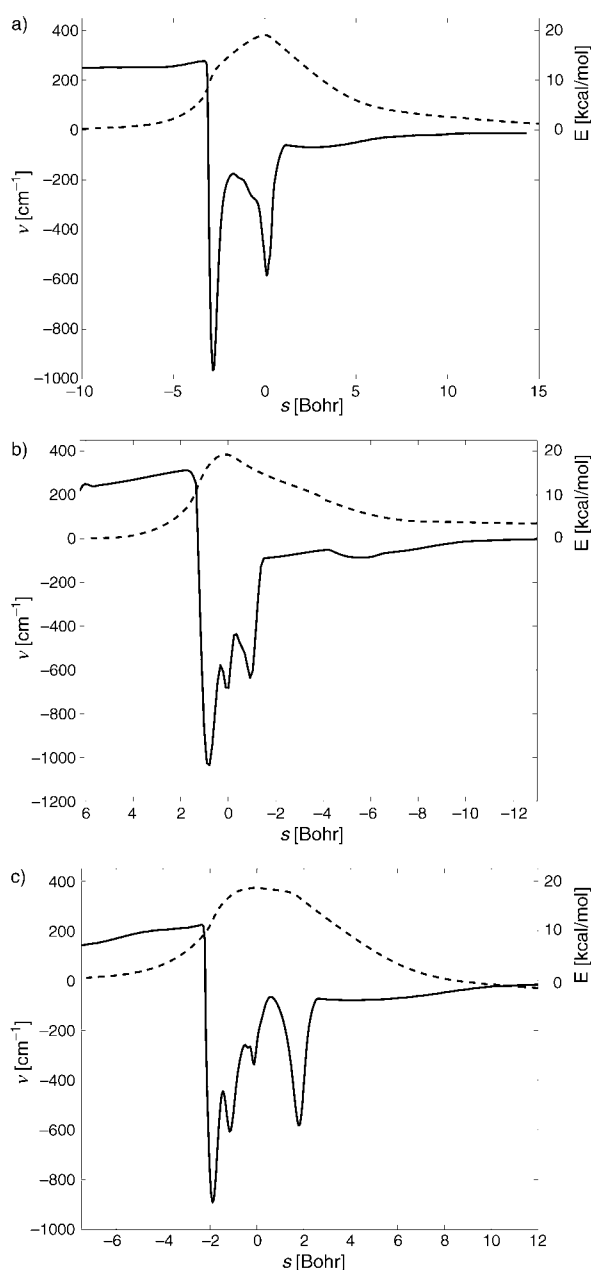


Figure 3. Imaginary frequencies (solid lines) and energy (dashed lines) along the reaction path of the decomposition of carbonic acid assisted by three water molecules. Top to bottom: reaction channels (a), (b), and (c). Imaginary numbers are depicted as negative due to a better presentability, and s is the reaction coordinate.

Reaction rates: As the reaction rates strongly depend on the energy barriers, they have to be determined very accurately when applying transition state theory. (As mentioned before a small change of $1.4 \text{ kcal mol}^{-1}$ within the barrier leads to a change in the reaction rate in the order of one magnitude at 300 K.) First we consider the reaction rates resulting from the CCSD(T) energy values, which were used for dual-level dynamics. These rates would correspond experimentally to a cluster of carbonic acid with three water molecules in the gas phase. The rates are depicted in Figure 4 together with previously published ones^[1] for better comparison.

When our calculations are compared with experimental rates it can be seen that they meet the experiment quite well in

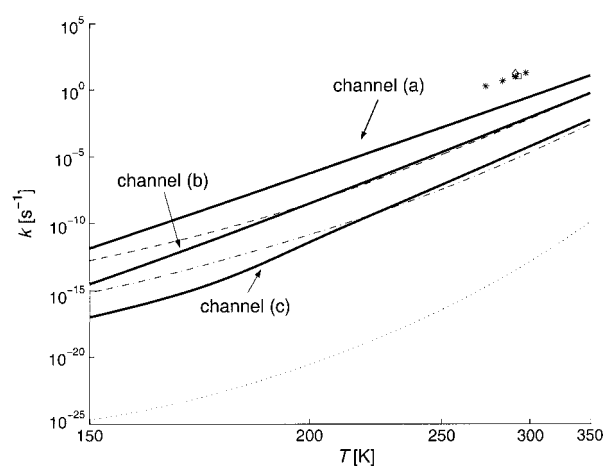


Figure 4. Reaction rates of the decomposition of carbonic acid with three additional water molecules via a) a six-membered, b) an eight-membered, and c) a 10-membered transition state. Comparison with experiment^[8, 7, 9] and earlier published results^[1] with fewer water entities is also given: (\cdots) no additional water molecules, ($-\cdot-\cdot-$) one additional water molecule, ($---$) two additional water molecules; (*) experimental values from Magid et al., (\diamond) experimental values from Roughton, (\square) experimental values from Meier et al.

the case of channel (a). At 20°C we predict a rate of 0.2 s^{-1} for reaction channel (a); this is in reasonable agreement with the experimental values of Meier et al. of 10 s^{-1} .^[8] Therefore, we have reduced the gap between experiment and theory by a factor 60 in comparison with our previous study. Astonishingly, there is just a factor of 50 missing to reach the experimental reaction rate in aqueous solution at 20°C .

Due to higher energy barriers, channels (b) and (c) yield reaction rates that are much lower than experimental ones. Especially, channel (c) reveals surprisingly low reaction rates, even lower than those of the decomposition reaction catalyzed by two water molecules. This may be explained by a significantly higher reaction barrier and a smaller tunneling correction due to heavy atom movement near the transition state. Therefore neither channel (b) nor (c) is able to compete with channel (a), and the mechanism via a six-membered ring may be proposed to be the most efficient one over the whole temperature range.

In contrast to the smaller systems ($n = 0, 1, 2$) tunneling does not play a very important role. At temperatures above 150 K the transmission factor κ (i.e., the enhancement of the reaction rate due to tunneling effects) is lower than 60 (in reaction channel (c) even lower than two). For comparison κ is about 10^{20} for the uncatalyzed decomposition of carbonic acid at 150 K. This may be explained by the narrower and much higher activation-energy barrier in that case.

Below 150 K in gas phase the mechanisms involving three water molecules lead to even lower reaction rates than the reactions catalyzed by fewer water entities. This implies that there is a significant change in the reaction mechanism due to tunneling effects on lowering the temperature.

Kinetic isotope effects: To have additional comparison with experiment, we calculated the kinetic isotope effects for the decomposition of deuterated carbonic acid catalyzed by $n = 0$,

Table 3. Kinetic isotope effects $k_{\text{H}_2\text{CO}_3}/k_{\text{D}_2\text{CO}_3}$ of the reaction $\text{H}_2\text{CO}_3 + n\text{H}_2\text{O} \rightarrow (n+1)\text{H}_2\text{O} + \text{CO}_2$.

T	$n=0$	$n=1$	$n=2$	$n=3(\text{a})$	$n=3(\text{b})$	$n=3(\text{c})$	exp. ^[a]
200 K	4.2×10^4	13	10	2.9	10	4.0	
300 K	220	3.4	3.0	2.2	3.0	2.7	≈ 2

[a] See ref. [6].

1, 2, 3 deuterated water molecules. Table 3 shows our results and the experimental one obtained by Pocker et al.^[6]

For the uncatalyzed system we predict a very high influence of isotopic substitution on the reaction rate, especially at low temperatures. Even at room temperature the KIE amounts to 220 and thus emphasizes the importance of tunneling even at higher temperatures. This means that the half-life of a deuterated carbonic acid monomer in the gas phase at room temperature is 40 million years (Recently, we determined the half-life for a carbonic acid molecule in the gas phase to be 0.18 million years.^[1]).

For the catalyzed reactions, a clear shift toward the experimental result can be found with an increasing number of water molecules. Three additional water molecules seem to be enough to approach the experimental value reasonably well. This gives evidence that at least three water molecules are required to explain the reaction mechanism in aqueous solution. Surprisingly, there are quite strong deviations of the different KIEs within the reactions employing three water molecules. While channel (a) approaches the experimental value quite well, channels (b) and (c) deviate strongly. This coincides with the observation that channel (a) reproduces the experimental reaction rates much better than the other possibilities.

Conclusion

When considering the decomposition of carbonic acid, the reaction barrier decreases significantly by increasing the number of additional catalytically active water entities. The uncatalyzed reaction has a barrier of $43.9 \text{ kcal mol}^{-1}$, addition of a single water molecule reduces it to $27.1 \text{ kcal mol}^{-1}$. More water molecules lead to a further decrease in the barrier, and we found the lowest barrier to be $20.9 \text{ kcal mol}^{-1}$ on participation of three additional water molecules.

Reaction rate calculations were done with variational Transition State Theory including quantum corrections. The reaction paths were determined at the B3LYP/6-31 + G(d) level of theory and were mapped in a dual level interpolation scheme onto high level (CCSD(T)/aug-cc-pVDZ) stationary points and frequencies (B3LYP/aug-cc-pVDZ). The investigations revealed at best a reaction rate of 0.2 s^{-1} at 20°C of carbonic acid with three water entities in the gas phase, with reaction channel (a).

Investigation of the KIEs of deuterated carbonic acid in deuterated water showed that they are in reasonable agreement with experiment when considering three water molecules.

Therefore, we propose a mechanism that goes via a six-membered transition state to be a possible dehydration

mechanism of carbonic acid in neutral aqueous solution at room temperature. The competing reactions via 8- and 10-membered transition states exhibit reaction rates 30 and 5000 times smaller, respectively, and are of minor influence. All mechanisms occur by a stepwise proton transfer chain and have a wide reaction barrier, so that tunneling does not play a very important role.

On lowering the temperature, tunneling is expected to become more relevant. Indeed, at about 125 K, the mechanisms with three water molecules yield lower rates than those with a smaller number of water molecules. This suggests that the dehydration mechanism changes completely at low temperatures, as tunneling compensates for the higher reaction barriers. At these temperatures, however, there is still lack of experimentally determined rate constants, and so far they can only be accessed by theoretical investigations like this one.

Acknowledgements

This work was supported by the Austrian Science Fund (Grant Number P14357-TPH). C.S.T. acknowledges support by the University of Innsbruck and T.L. by the Austrian Academy of Sciences.

- [1] T. Loerting, C. Tautermann, R. T. Kroemer, I. Kohl, A. Hallbrucker, E. Mayer, K. R. Liedl, *Angew. Chem.* **2000**, *112*, 919–922; *Angew. Chem. Int. Ed.* **2000**, *39*, 891–894.
- [2] D. N. Silverman, S. Lindsog, *Acc. Chem. Res.* **1988**, *21*, 30–36.
- [3] D. N. Silverman, *Methods Enzymol.* **1995**, *249*, 479–503.
- [4] A. S. Fauci, E. Braunwald, K. J. Isselbacher, J. D. Wilson, J. B. Martin, D. L. Kasper, S. L. Hauser, D. L. Longo, *Harrison's Principles of Internal Medicine, 14th ed.*, McGraw Hill, New York, **1998**.
- [5] Y. Pocker, N. Janjic, *J. Am. Chem. Soc.* **1989**, *111*, 731–733.
- [6] Y. Pocker, D. W. Bjorkquist, *J. Am. Chem. Soc.* **1977**, *99*, 6537–6543.
- [7] E. Magid, B. O. Turbeck, *Biochim. Biophys. Acta* **1968**, *165*, 515–524.
- [8] J. Meier, G. Schwarzenbach, *Helv. Chim. Acta* **1957**, *40*, 907–917.
- [9] F. J. W. Roughton, *J. Am. Chem. Soc.* **1941**, *63*, 2930–2934.
- [10] J. F. Marlier, M. H. O'Leary, *J. Am. Chem. Soc.* **1984**, *106*, 5054–5057.
- [11] B. Jönsson, G. Karlström, H. Wennerström, B. Roos, *Chem. Phys. Lett.* **1976**, *41*, 317–320.
- [12] B. Jönsson, G. Karlström, H. Wennerström, S. Forsen, B. Roos, J. Almlöf, *J. Am. Chem. Soc.* **1977**, *99*, 4628–4632.
- [13] K. R. Liedl, S. Sekusak, E. Mayer, *J. Am. Chem. Soc.* **1997**, *119*, 3782–3784.
- [14] C. A. Wight, A. I. Boldyrev, *J. Phys. Chem.* **1995**, *99*, 12125–12130.
- [15] J. Sadlej, P. Mazurek, *J. Mol. Struct.* **1995**, *337*, 129–138.
- [16] K. M. Merz, Jr., *J. Am. Chem. Soc.* **1990**, *112*, 7973–7980.
- [17] W. Hage, K. R. Liedl, A. Hallbrucker, E. Mayer, *Science* **1998**, *279*, 1332–1335.
- [18] M. T. Nguyen, G. Raspoet, L. G. Vanquickenborne, P. T. Van Duijnen, *J. Phys. Chem. A* **1997**, *101*, 7379–7388.
- [19] M. H. Moore, R. K. Khanna, *Spectrochim. Acta* **1991**, *47A*, 255–262.
- [20] J. R. Brucato, M. E. Palumbo, G. Strazzula, *Icarus* **1997**, *125*, 135–144.
- [21] W. Hage, A. Hallbrucker, E. Mayer, *J. Am. Chem. Soc.* **1993**, *115*, 8427–8431.
- [22] P. A. Gerakines, M. H. Moore, R. L. Hudson, *Astron. Astrophys.* **2000**, *357*, 793–800.
- [23] G. Strazzulla, J. R. Brucato, G. Cimino, M. E. Palumbo, *Planet. Space Sci.* **1996**, *44*, 1447–1450.
- [24] M. Zuber, D. E. Smith, S. C. Solomon, J. B. Abshire, R. S. Afzal, O. Aharoson, K. Fishbaugh, P. G. Ford, H. V. Frey, J. B. Garvin, J. W. Head, A. B. Ivanov, C. L. Johnson, D. O. Muhleman, G. A. Neumann, G. H. Pettengill, R. J. Phillips, X. Sun, H. J. Zwally, W. B. Banerdt, T. C. Duxbury, *Science* **1998**, *282*, 2053–2060.
- [25] B. M. Jakosky, *Science* **1999**, *283*, 648–649.

- [26] J. M. Lyons, J. Corish, *Corros. Sci.* **1996**, *38*, 1331–1356.
- [27] S. Charbonneau, R. Gilbert, L. Lépine, *Anal. Chem.* **1995**, *67*, 1204–1209.
- [28] *CO₂ Capture, Reuse, and Storage Technologies for Mitigating Global Climate Change*, Energy Laboratory, Massachusetts of Technology, January **1997**.
- [29] H. Herzog, E. Adams, M. Akai, G. Alendal, L. Golment, P. Haugan, S. Masuda, R. Matear, S. Masutani, T. Ohsumi, C. S. Wong, *Update on the International Experiment on CO₂ Ocean Sequestration, 5th International Conference on Greenhouse Gas Control Technology*, Cairns, Australia, August **2000**.
- [30] R. Dalton, *Nature* **1999**, *401*, 315.
- [31] P. M. Haugan, H. Drange, *Energy Convers. Manage.* **1996**, *37*, 1019–1022.
- [32] G. Stegen, K. Cole, *Energy Convers. Manage.* **1995**, *36*, 497–500.
- [33] M. Eigen, K. Kustin, G. Maass, *Z. Phys. Chem.* **1961**, *30*, 130–136.
- [34] H. Eyring, *J. Chem. Phys.* **1935**, *3*, 107–115.
- [35] B. C. Garret, D. G. Truhlar, *J. Chem. Phys.* **1983**, *79*, 4931–4938.
- [36] D. G. Truhlar, B. C. Garrett, *Ann. Rev. Phys. Chem.* **1984**, *35*, 159–189.
- [37] B. C. Garrett, T. Joseph, T. N. Truong, D. G. Truhlar, *Chem. Phys.* **1989**, *136*, 271–283.
- [38] A. Gonzalez-Lafont, T. N. Truong, D. G. Truhlar, *J. Chem. Phys.* **1991**, *95*, 8875–8894.
- [39] R. T. Skodje, D. G. Truhlar, B. C. Garret, *J. Phys. Chem.* **1981**, *85*, 3019–3023.
- [40] D. G. Truhlar, A. D. Isaacson, B. C. Garrett, in *Theory of Chemical Reaction Dynamics* (Ed.: M. Baer), *Generalized Transition State Theory*, CRC Press, Boca Raton, FL, **1985**, pp. 65–137.
- [41] S. C. Tucker, D. G. Truhlar, J. Bertran, I. G. Csizmadia, in *New Theoretical Concepts for Understanding Organic Reactions* (Eds.: J. Bertran, I. Csizmadia), *Dynamical Formulation of Transition State Theory: Variational Transition States and Semiclassical Tunneling*, Kluwer, **1989**, pp. 291–346.
- [42] M. Page, J. W. McIver, *J. Chem. Phys.* **1988**, *88*, 922–935.
- [43] V. S. Melissas, D. G. Truhlar, B. C. Garrett, *J. Chem. Phys.* **1992**, *96*, 5758–5772.
- [44] J. A. Pople, M. Head-Gordon, D. J. Fox, K. Raghavachari, L. A. Curtiss, *J. Chem. Phys.* **1989**, *90*, 5622–5629.
- [45] L. A. Curtiss, K. Raghavachari, G. W. Trucks, J. A. Pople, *J. Chem. Phys.* **1991**, *94*, 7221–7230.
- [46] Y. Kim, *J. Am. Chem. Soc.* **1996**, *118*, 1522–1528.
- [47] W.-P. Hu, Y.-P. Liu, D. G. Truhlar, *J. Chem. Soc. Faraday Trans.* **1994**, *90*, 1715–1725.
- [48] M. Child, *Semiclassical Mechanics with Molecular Applications*, Clarendon, Oxford, **1991**.
- [49] R. T. Skodje, D. Truhlar, *J. Chem. Phys.* **1982**, *77*, 5955–5976.
- [50] A. Fernandez-Ramos, D. G. Truhlar, *J. Chem. Phys.* **2000**, *114*, 1491–1496.
- [51] Y.-P. Liu, D.-H. Lu, A. Gonzalez-Lafont, D. G. Truhlar, B. C. Garrett, *J. Am. Chem. Soc.* **1993**, *115*, 7806–7817.
- [52] *Gaussian 98* (Revision A.7), M. J. Frisch, G. W. Trucks, H. B. Schlegel, G. E. Scuseria, M. A. Robb, J. R. Cheeseman, V. G. Zakrzewski, J. A. Montgomery, R. E. Stratmann, J. C. Burant, S. Dapprich, J. M. Millam, A. D. Daniels, K. N. Kudin, M. C. Strain, O. Farkas, J. Tomasi, V. Barone, M. Cossi, R. Cammi, B. Mennucci, C. Pomelli, C. Adamo, S. Clifford, J. Ochterski, G. A. Petersson, P. Y. Ayala, Q. Cui, K. Morokuma, D. K. Malick, A. D. Rabuck, K. Raghavachari, J. B. Foresman, J. Cioslowski, J. V. Ortiz, B. B. Stefanov, G. Liu, A. Liashenko, P. Piskorz, I. Komaromi, R. Gomperts, R. L. Martin, D. J. Fox, T. Keith, M. A. Al-Laham, C. Y. Peng, A. Nanayakkara, C. Gonzalez, M. Challacombe, P. M. W. Gill, B. G. Johnson, W. Chen, M. W. Wong, J. L. Andres, M. Head-Gordon, E. S. Replogle, J. A. Pople, Gaussian, Inc., Pittsburgh PA, **1998**.
- [53] *Polyrate 8.5*, Y.-Y. Chuang, J. C. Corchado, P. L. Fast, J. Villá, E. L. Coitiño, W.-P. Hu, Y.-P. Liu, G. C. Lynch, K. A. Nguyen, C. F. Jackels, M. Z. Gu, I. Rossi, S. Clayton, V. S. Melissas, R. Steckler, B. C. Garrett, A. D. Isaacson, D. G. Truhlar, University of Minnesota, Minneapolis, **2000**.
- [54] *Gaussrate 8.5*, J. C. Corchado, E. L. Coitiño, Y.-Y. Chuang, D. G. Truhlar, University of Minnesota, Minneapolis, **2000**.
- [55] T. Loerting, K. R. Liedl, B. M. Rode, *J. Chem. Phys.* **1998**, *109*, 2672–2679.
- [56] W.-K. Li, M. L. McKee, *J. Phys. Chem. A* **1997**, *101*, 9778–9782.
- [57] T. Loerting, K. R. Liedl, *Proc. Natl. Acad. Sci. USA* **2000**, *97*, 8874–8878.
- [58] R. Steudel, *Angew. Chem.* **1995**, *107*, 1433–1435; *Angew. Chem. Int. Ed. Engl.* **1995**, *107*, 1313–1315.
- [59] L. J. Larson, M. Kuno, F. M. Tao, *J. Chem. Phys.* **2000**, *112*, 8830–8838.
- [60] T. Loerting, R. T. Kroemer, K. R. Liedl, *Chem. Commun.* **2000**, 999–1000.
- [61] J. P. McNamara, I. H. Hillier, *J. Phys. Chem. A* **2000**, *104*, 5307–5319.
- [62] Y. Kim, H. J. Hwang, *J. Am. Chem. Soc.* **1999**, *121*, 4669–4676.
- [63] Z. Smedarchina, W. Siebrand, A. Fernandez-Ramos, L. Gorb, J. Leszczynski, *J. Chem. Phys.* **2000**, *112*, 566–573.
- [64] D. E. Folmer, E. S. Wisniewski, J. R. Stairs, A. W. Castleman, Jr., *J. Phys. Chem. A* **2000**, *104*, 10545–10549.
- [65] J.-H. Lim, E. K. Lee, Y. Kim, *J. Phys. Chem. A* **1997**, *101*, 2233–2239.
- [66] H. Eyring, *J. Chem. Phys.* **1935**, *3*, 107–115.
- [67] K. J. Laidler, M. C. King, *J. Phys. Chem.* **1983**, *87*, 2657–2664.
- [68] D. G. Truhlar, W. L. Hase, J. T. Hynes, *J. Phys. Chem.* **1983**, *87*, 2664–2682.
- [69] E. Wigner, *Z. Phys. Chem. B* **1932**, *32*, 203–216.
- [70] W. H. Miller, *Faraday Discuss.* **1976**, *62*, 40–46.
- [71] R. A. Marcus, E. Coltrin, *J. Chem. Phys.* **1977**, *67*, 2609–2613.
- [72] V. Barone, M. Cossi, J. Tomasi, *J. Comput. Chem.* **1998**, *19*, 404–417.

Received: May 25, 2001 [F3285]